sciendo
Austrian Journal of Earth Sciences | Vienna | 2019 | Volume 112/2 | 84 - 102 | DOI: 10.17738/ajes.2019.0006

Evidence for pre-Pleistocene landforms in the Eastern Alps: Geomorphological constraints from the Gurktal Alps

Thorsten BARTOSCH[1)*)] & Kurt STÜWE[1)]

[1)] Institute of Earth Sciences, University of Graz, Universitätsplatz 2, A-8010, Graz, Austria

[*)] Corresponding author: thorsten.bartosch@uni-graz.at

KEYWORDS geomorphology, palaeo-surfaces, Gurktal, Eastern Alps

Abstract

We present evidence for a series of pre-Pleistocene landforms on hand of a new geomorphological map for the Gurktal region of the Eastern Alps. The Gurktal Alps region is the westernmost region of the Eastern Alps that escaped the glacial reshaping in the Pleistocene. Its morphology therefore preserves evidence of older landforms in closer proximity to the central part of the range than any other region in the Alps. The region is therefore useful to document aspects of the geomorphological evolution for the Eastern Alps during both, the Pleistocene glaciations and the earlier uplift history. Our mapping approach is twofold. We applied stream-power analysis outside the glacially overprinted areas to detect and classify spatially distinct quasi-stable stream segments, which we expanded to planar objects using slope analysis combined with field mapping. Our mapping results document four palaeo-surfaces located roughly at about 1500 m, 1200 m, 900 m and about 800 m above sea level. We correlate these levels with well-known palaeo-surfaces from the eastern end of the Alps and suggest that they can be interpreted in terms of more than 1000 m of surface uplift in the last six million years. Channel analysis and the distribution of Pleistocene gravel terraces suggest that the main trunk of the river Gurk was diverted from the Wimitz valley in the Rissian. Furthermore, steam-power analysis documents an ongoing activity of the Görschitztal fault and some inferred Pleistocene activity of a north-west trending fault close to the township of Gurk.

1. Introduction

The morphological evolution of the Eastern Alps is not very well known, but is generally believed to have started in the Oligocene from a hilly lowland topography (Frisch et al., 1998). This interpretation is based on the age of the oldest sediments in the molasse foreland basins (Kuhlemann et al., 2006; Kuhlemann and Kempf, 2002), on abundant geochronological information from both detritus and basement studies (Spiegel et al., 2001; Wölfler et al., 2012) and on some indirect evidence from palaeo-surfaces. In particular, the elevated karst plateaus of the Northern Calcareous Alps (at around 2000 m elevation in the Tennengebirge, Dachstein and Hochschwab), have been used as a proxy for the uplift history as they preserve sedimentary remnants of low-lying braided river systems (Augenstein Formation; Frisch et al., 2001).

However, there is also a series of other, lower palaeo-surfaces that have been recognized in the Eastern Alps, but have received comparably little attention for interpreting the uplift history. These include levels from, for example, the Koralpe and the Grazer Bergland (Legrain et al., 2014; Wagner et al., 2010), or the Nockalm surface (Exner et al., 1949; Winkler-Hermaden, 1957) and other places in the Niedere Tauern Region (Dertnig et al., 2017). Many of these surfaces lie well-outside the ice sheets of the glaciation periods and they are clearly relics of pre-Pleistocene base levels. Their current, elevated position in several discrete levels up to 1500 m above current base level has been interpreted as evidence for a young (potentially post-Miocene) surface uplift event (Legrain et al., 2014; Wagner et al., 2010). This event has also been recognized in the erosion of the Molasse basins (Genser et al., 2007; Baran et al., 2014), the Styrian basin (Ebner and Sachsenhofer, 1995; Dixon et al., 2016), in the Malé Karpaty Mts. (Western Carpathians) in western Slovakia (Šujan et al., 2017) and at the western (Ruszkiczay-Rüdiger et al., 2011) and southern margins (Ruszkiczay-Rüdiger et al., 2018) of the Transdanubian Range within the Pannonian basin. The understanding of this young uplift is still in its infancy, details of the timing badly constrained and its extent is largely unknown. In order to trace geomorphological evidence for this uplift event towards the west, much of the Eastern Alps are of little use as glaciation has substantially re-sculpted the range (van Husen, 1987). To understand this event it is therefore useful to study the geomorphology of the westernmost regions of the Eastern Alps that escaped glaciation in the Pleistocene. We focus our study on the Gurktal region as an example (Fig. 1).

In this paper we present the results of a geomorphological mapping project in the Gurktal Alps. We present a new geomorphological map for the region and derive evidence for a series of pre-Pleistocene palaeo-surfaces in the region. In our discussion we correlate the palaeo-surfaces with well-known palaeo-surfaces in the Grazer Bergland and use this interpretation to infer aspects

about the timing and the extent of post-Miocene surface uplift in the Eastern Alps.

2. Geology and Geomorphology of the Gurktal Alps

The Gurktal Alps are a moderately mountainous area in the Eastern Alps that was located in an ice-free oasis during the glaciation periods. It was almost entirely surrounded by the Pleistocene ice-shield (Fig. 1a, see map in van Husen (1987)). The Gurktal Alps are confined by the Niedere Tauern and the Klagenfurter basin to the north and south and by the Saualpe / Seetal Alps and the eastern edge of the Tauern Window to the

Figure 1: Location map of the Gurktal Alps and their position in the context of the Pleistocene extent of glaciation. A: Shows the LGM extent (van Husen, 2012) on top of a DEM (Cooperation OGD Austria, 2015) of the Eastern Alps together with fault systems bordering the Gurktal Block in Central Carinthia and the investigation area within the not glacially overprinted Gurktal Alps. B: Overview of sub-massifs in the Gurktal Alps and the related river systems overlain by the LGM extent (van Husen, 2012). The red circles with captial letter indices are showing the approximate locations of the field photographs in Fig. 5.

east and west, respectively. Topographic heights vary between 440 m at the Wörthersee and about 2400 m high mountains in the north-west (the Nock Mountain peaks of Rosennock, Eisenhut). The Gurk, the Metnitz, the Wimitz and the Görschitz form the major drainages of the region. During the last glacial maximum (LGM: between 25–24 ka according to van Husen, 2011), the eastward flowing Mur and Drau glaciers flanked major parts of the investigation area.

Geologically, the Gurktal Alps are made up of amphibolite-facies crystalline rocks (Neubauer and Pistotnik, 1984), overlain by Palaeozoic phyllites of the Gurktal nappe complex (Neubauer and Pistotnik, 1984; Rantitsch and Russegger, 2000) (Fig. 2). The crystalline basement is exhumed within several tectonic windows. East of the Gurk river and downstream of Althofen, upper Cretaceous sediments (Krappfeld-Gosau) transgress an erosional surface on top of the Gurktal nappes (Neumann, 1989). Apatite fission-track ages from the northern and western margin of the Gurktal Alps (Hejl, 1997, 1998; Reinecker, 2000) suggest exhumation of the metamorphic rocks in the early Miocene with denudation rates around 87 m/Ma from 34–23 Ma, followed by a mid-Miocene phase of stagnation. The Miocene exhumation history is paralleled by the formation of the terrestrial Tamsweg basin to the north-west of the studied region (Aigner, 1924; Zeilinger et al., 1999) and probably the peneplanation of the Nockalm surface. A final phase of Plio- to Pleistocene rapid cooling phase (~4 Ma) is suggested (Hejl, 1997, 1998; Reinecker, 2000). Finally, Neubauer et al. (2018) investigated the Reifnitz tonalite to the south of the Wörthersee, about 30 km southward of our investigation area. They recognize a Late Oligocene exhumation followed by a final Late Miocene to Pliocene exhumation phase of the Wörthersee antiform.

2.1 Geomorphology and landscape evolution

The "Gurktal Block" is the neotectonic unit that governs the landscape evolution (Frisch et al., 1998; Reinecker, 2000; Wölfer et al., 2011) in the region of interest. It completely comprises the investigation area and is bordered by the north-west trending Pöls-Lavanttal, Radenthein strike-slip the south-west orientated Katschberg normal fault and the east-west directed Prebersee and Seetal faults (westernmost section of the Mur-Mürz fault) (Fig. 1a). This block is supposed to have slid down relative to the northern regions by about 1000 m in south-south-east direction in the Middle Miocene (Reinecker, 2000; Wölfler et al., 2011) during the phase of lateral extrusion of the Eastern Alps (Ratschbacher et al., 1991), resulting in a topographic low. This was also resolved by landscape evolution modelling in Bartosch et al. (2017).

The Nockalm surface (at around 1700–2200 m surface elevation) is the highest, oldest and best known

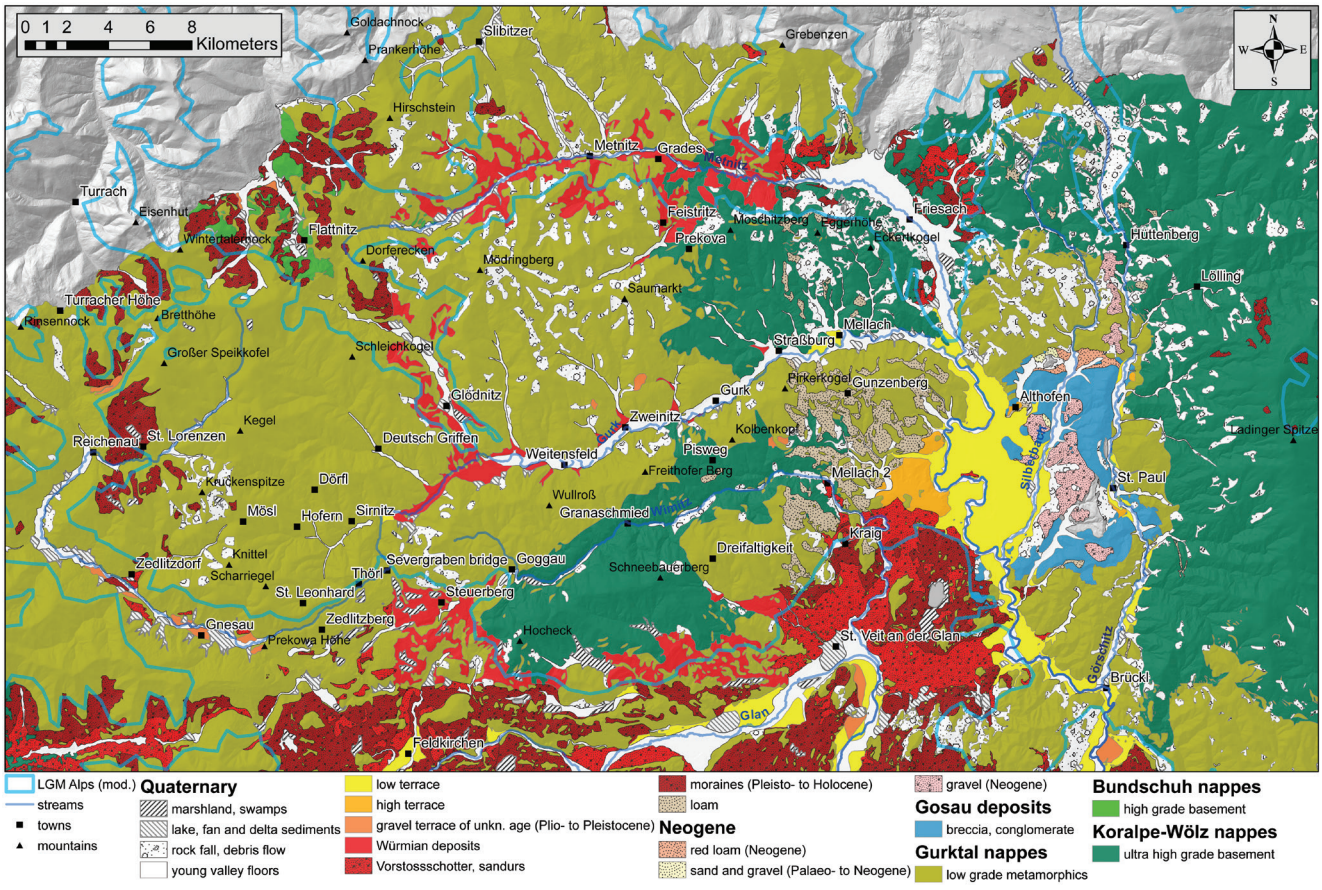

Figure 2: Simplified geological map of the Gurktal Alps (GeoServices-KAGIS, 2017) and the modified LGM extent is shown (light blue line).

palaeo-surface of the Gurktal Block (Exner, 1949). Its planation is interpreted to coincide with the motion of the Gurktal Block during the phase of stagnation of the exhumation in the Miocene (Reinecker, 2000; Wölfler et al., 2011). It forms one of the early stages of the landscape evolution of the Gurktal Alps. Although it is glacially overprinted, this planation surface is still clearly recognized from the east of the Katschberg fault to the Flattnitz depression (Paalbach valley to the north of Flattnitz village, see Fig. 1b) in the northwestern part of the Nock Mountains. It consists out of hard-rock summit plateaus, (e.g. the Aineck close to the Katschberg) and large swampy peneplains with some preserved red loam palaeo-soils (Exner, 1989; Exner et al., 2005). Possibly related red loams are also found in the Gurktal region at the northern border of the Althofen basin (Fig. 2) and at its southwestern margin in the vicinity of Gunzenberg (Neubauer, pers. com., 2018).

South of the Nock Mountains and its planation surface, the topography of the Gurktal Alps descends in several steps from the Niedere Tauern toward the Klagenfurt basin. Aigner, (1922) suggested already that this may be interpreted in terms of a descending Piedmont-step landscape, where different levels developed during phases of tectonic stasis (Spreitzer, 1932). In the centre of this rather erosion-protected Gurktal Block, the Nock Mountains depression constitutes a circular crater-like structure of approximately 40 km diameter (white circle in Fig. 1b). In contrast to the surrounding ridges, the Metnitz, the Mödring and the Wimitz Mountains (Zammelberg and Schneebauer Ridge) inside the Nock Mountains depression are striking in east-north-east direction and are about 500 m lower than mountains outside the depression. No faults or lithological changes are known that control the lower morphology of the Nock Mountains depression.

The final phase of surface uplift and denudation of the region in the Plio- and Pleistocene was accompanied by the glaciation periods. While much of the Gurktal region remained ice-free, evidence for glacially-derived deposits is abundant. Pleistocene higher and lower sandurs are deposited to the south of Friesach and along main parts of the Gurk channel (see Fig. 2, 3). In particular within the Althofen basin the succession starts with several low terrace levels with steps in the range of 2–5 m. The Würmian low terrace sediments are the most widespread terraces in the region. They range from altitudes around 835–760 m at both sides of the Gurk river at Albeck castle close to Sirnitz, further down to the Glödnitz junction. Remnants of these terraces are still preserved at the left bank of the Gurk between Weitensfeld and Mellach and they become widespread within vast areas extending to both sides of the Gurk river bank below the junction with the Metnitz river (640–550 m). No traces of low terrace sediments are found along the Wimitz- and Metnitz rivers. Above the low terrace deposits the only remnants of a Rissian high terrace are isolated at a height of 581–709 m at the western border of the Althofen basin.

3. Methods

In order to map the geomorphology of the Gurktal Alps, we applied a combined approach using numerical analysis of a digital elevation models combined with field work. In particular, we used a fluvial incision model to identify knick-points in rivers in both main trunks and tributary streams. For the incision model we follow the "stream power approach" where the geomorphic steady state channel profile of fluvial channels is described by:

$$S = \left(\frac{u}{k}\right)^{1/n} A^{-m/n} = k_s A^{-\theta} \quad (1)$$

where S is local slope, A is the catchment area (as a proxy for water flux), u is the rock uplift rate and k the erodibility of the bedrock. Then the steepness index is defined as $k_s = (u/k)^{1/n}$ and the concavity index is given by $\theta = m/n$. The exponents n and m describe the relative contributions of slope and catchment area to erosion (Hergarten et al., 2016; Kirby et al., 2003; Whipple and Tucker, 1999; Wobus et al., 2006; Howard and Kerby, 1983). This equation is also referred to as Hack's law (Hack, 1957). In a double logarithmic plot of slope (S) against catchment area (A), equilibrium channels according to eq. (1) show a linear correlation and departures from this data set are interpreted as knick-points.

For the Gurktal Alps analysis the pour point is chosen at the junction with the Drau river. As most analysed channels in the Gurktal region show strong disequilibrium features with several knick-points along the channels, equilibrium sections of the individual channels can only be identified for small segments. In order to identify such segments, a log(A) - log(S) regression model in eq. (1) is computed based on a histogram of 200 bins/decade for A for the estimation of θ. The k_s parameter is estimated on a χ transformed (Perron and Royden, 2013; Royden and Perron, 2013) model of eq. (1), which results in considerably tighter and symmetric confidence intervals. With the derived k_s and θ parameters, profiles for the inferred equilibrium channel segments were calculated. Each equilibrium segment, with a knick-point close to its lower regression data range is interpreted as an upward travelling stationary river segment (Fig. 4). In this case, the elevation of the downstream extrapolation of the fitted channel profile above the channel may be used a proxy of incision between a relict and incised landscape (Legrain et al., 2014) or as the proxy for the elevation of a palaeo-surface if negligible erosion on these plains is assumed (see values in Table 1, 2). These discontinuities are recognized only strongly blurred in DEMs and in the field in the present study region. Some of the reasons for this are illustrated in the schematic geomorphological evolution model in Fig. 4. The picture shows a succession of varying uplift periods (or uplift and stasis as an extreme) and its effect to the main trunk cross-section (left hand side) and the river profile of a connected tributary (right hand side).

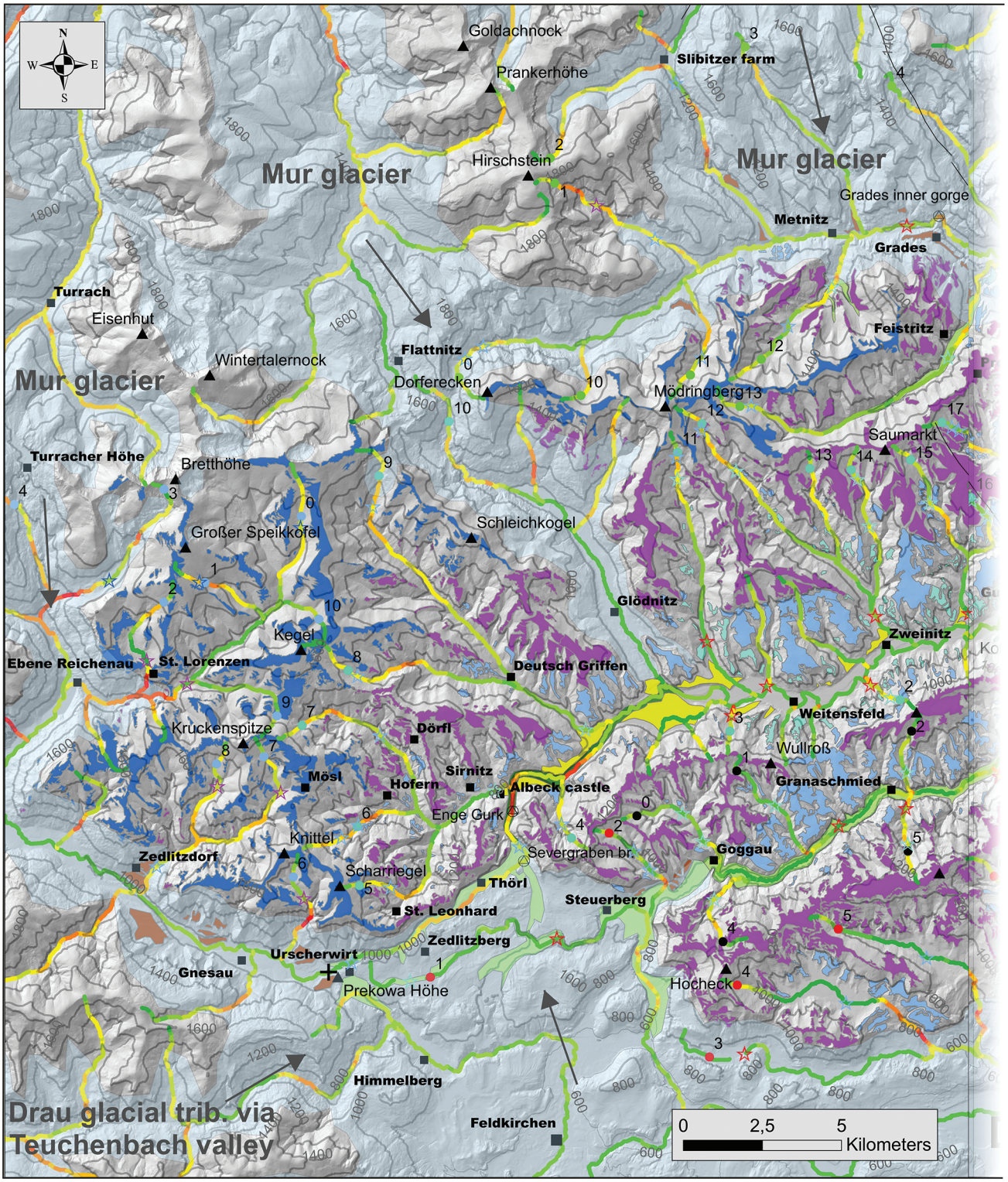

LGM Alps (mod.)
palaeoglacial flow
faults
geograph. feat.
towns
villages
mountains
level ref. points

Gurk upper tributaries
0, Gurk
1, Neuwirtalmbach
2, Andertalbach
3, Saureggenbach
4, Holzbodenbach
6, Peiningbach
7, Görzbach
8, Kotzgrabenbach
9, Ursulabach
10, Stoicharthüttenb.

Metnitz tributaries
0, Metnitz
1, Schwarzenb.
2, Röttingbach
3, Teichlbach
4, Rossbach
10, Ulsbach
11, Mödringb. 2
12, Vellachbach
13, Feistritz

Middle Gurk tributaries
2, Hafendorfbach
3, Zammelsbergbach
4, Albeck o. Schattseit.
5, Leonhardsbach
6, Sirnitz
7, Stronbach
8, Hochrindlbach
9, Griffenbach
10, Glödnitz
11, Mödringbach
12, Zweinitzenbach
13, Plötschgrabenb.
14, Krassnitzbach
15, Mühlbachgraben
16, Draschelbach
17, Langwiesenbach

Wimitz tributaries
0, Wimitz
1, Frischgraben
2, Pitschgraben
4, Graibach
5, Steinbichelbach

Glan tributaries
1, Roggbach
2, Bachergrabenb.
3, Liembergbach
4, Feitritz2
5, Harterbach

Figure 3: Interpreted geomorphological map of the Gurktal Alps showing the mapped palaeo-surfaces L_1–L_4 together with Pleistocene glacial information and analysed knick-point locations and k_{sn} values. Reference points for stream power analysis are displayed as "+" for each catchment.

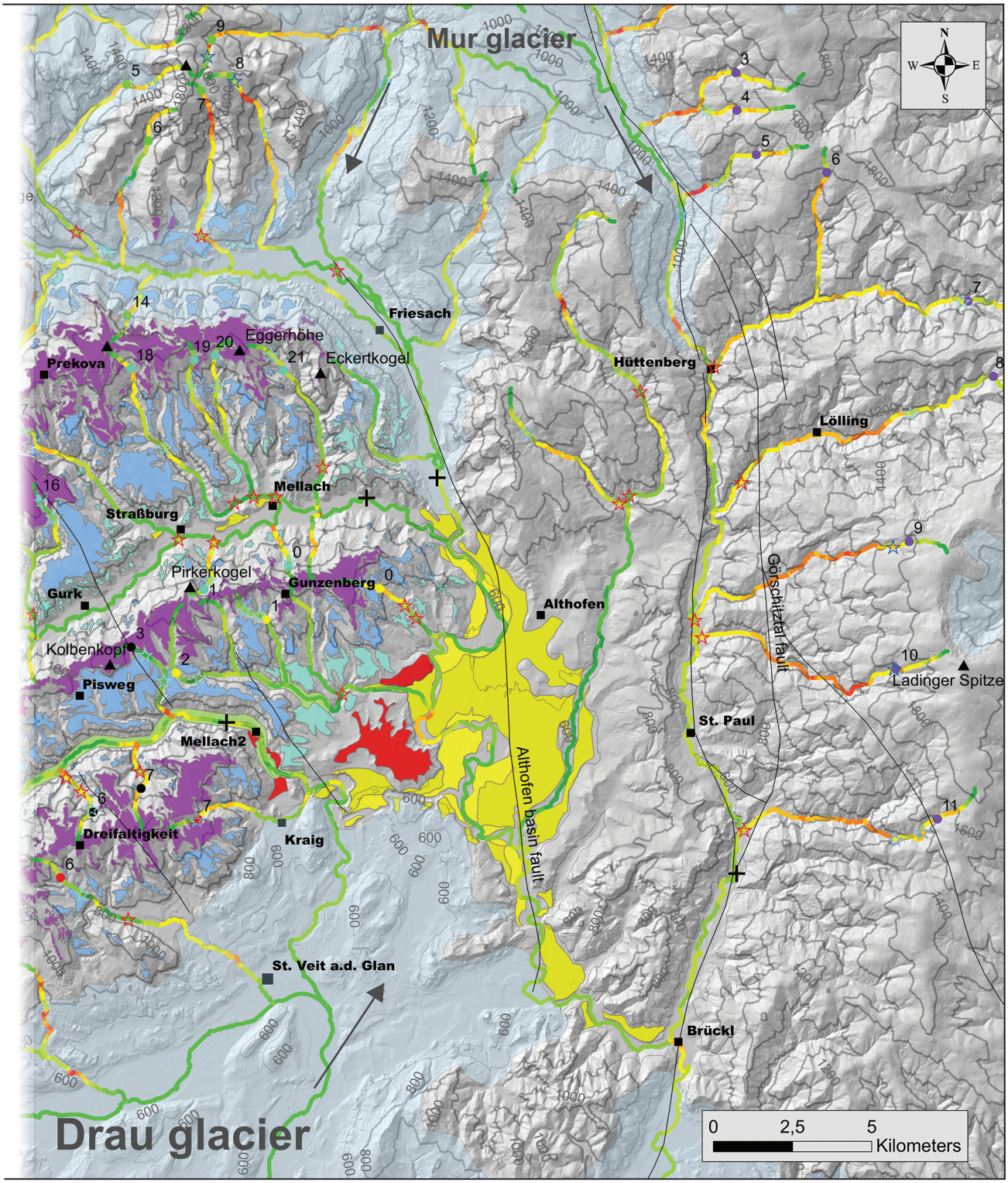

Metnitz tributaries
- 5, Gwerzbach
- 6, Moserwinklb.
- 7, Timrianbach
- 8, Schranzbach
- 9, Pöllauerbach
- 14, Zienitzenbach

Wimitz tributaries
- 3, Schwarzenbach2
- 6, Goschenbach
- 7, Gritschgrabenb.

Lower Gurk tributaries
- 0, Rabingbach
- 1, Watteinbach
- 2, Zabersdorfbach

Middle Gurk tributaries
- 0, Kainzbach
- 1, Pirkerkogelbach
- 16, Draschelbach
- 18, Ratschachbach
- 19, Wildbachgraben
- 20, Olschnöggbach
- 21, Höllgrabenbach

Görschitz tributaries
- 3, Tiefenbach
- 4, Hörbach
- 5, Hinterbergbach
- 6, Schafgrabenbach
- 7, Mosinzbach
- 8, Löllingbach
- 9, Greierbach
- 10, Grünburgerbach
- 11, Driesseckerbach

Glan tributaries
- 6, Mühlbach
- 7, Kraigerbach

knick-pts.
- L0
- L1
- L2
- L3
- L4

ksn
- 0 - 25
- 25 - 35
- 35 - 50
- 50 - 70
- 70 - 100
- 100 - 140
- 140 - 200
- 200 - 280
- 280 - 650

Planation surfaces
- post-glacial incision
- low terrace 1
- low terrace 2
- unk. terrace (post-gl.?)
- inter-glacial carve
- high terrace L0
- palaeo-surface L1
- palaeo-surface L2
- palaeo-surface L3
- palaeo-surface L4

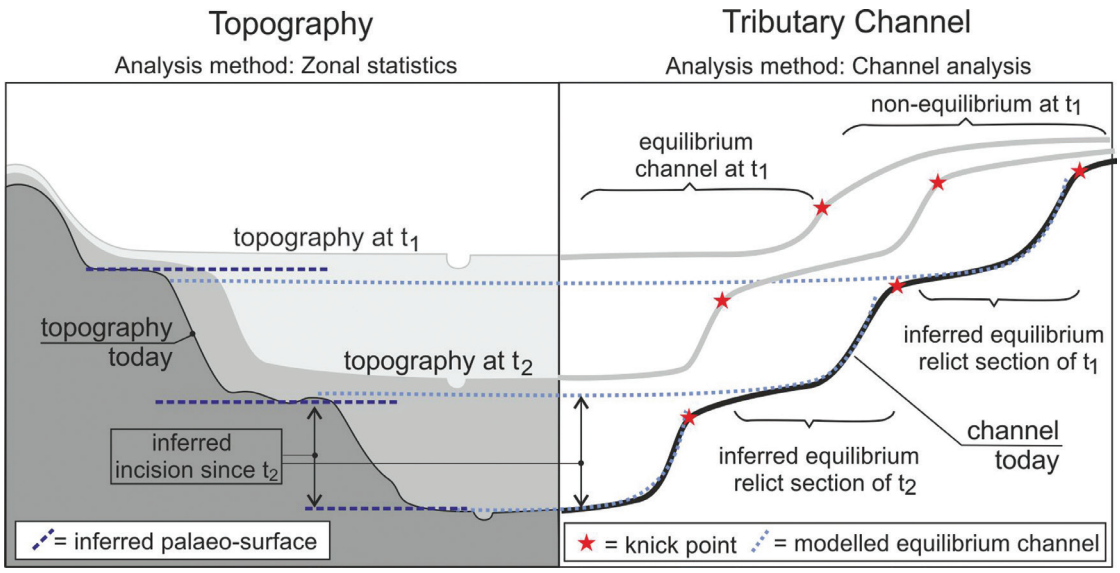

Figure 4: Schematic geomorphological evolution model of a landscape that is incised by rivers and successively uplifted with varying rates. Snapshots of the topography at three distinct times, which relate to a succession of varying uplift periods (or uplift and stasis as an extreme). Accordingly, the development of terraces in the main trunk cross-section (left hand side) and steps in the river profile of a connected tributary (right hand side) can be observed.

river system	level	x_{ref} [km]	$h_m \pm \sigma$ [m]	$h_{inc} \pm \sigma$ [m]	min-max [m]
Upper Gurk	L0	131	-	-	-
	L1	131	-	-	-
	L2	131	969±13	29±13	960-978
	L3	131	1213±41	273±41	1134-1268
	L4	131	1498±48	558±48	1464-1532
Middle Gurk	L0	82	664±39	56±39	616-731
	L1	82	764±38	156±38	675-822
	L2	82	913±41	305±41	860-997
Metnitz	L0	81	647±0	38±0	647-647
	L1	81	779±10	170±10	772-786
	L2	81	914±41	305±41	854-988
	L3	81	1183±0	573±0	1183-1183
	L4	81	1453±82	844±82	1395-1511
Wimitz	L0	60	706±28	104±28	672-732
	L1	60	767±33	165±33	709-803
Silberbach	L0	60	617±0	49±0	617-617
	L1	60	809±0	241±0	809-809
	L2	60	961±46	392±46	928-994
Görschitz	L0	50	594±27	39±27	566-620
	L1	50	746±31	191±31	719-780
	L2	50	996±28	441±28	972-1027
	L3	50	-	-	-
	L4	50	1531±27	976±27	1512-1550

Table 1: Statistics of levels L_0–L_4 as derived from channel analysis of all studied tributaries to the main drainage listed in the first column. h_m is the mean elevation (and its confidence interval) of all modelled equilibrium segments of channel profiles (from Fig. 7) at position x_{ref} of the main trunk as shown by the cross on Fig. 3 or 7. h_{inc} is the elevation difference between h_m and the elevation of x_{ref} and may be interpreted as the amount of base level incision, following the formation of the corresponding level. A comparison of the levels (h_m) across the six different considered catchments reveals a fairly good correlation between absolute altitudes for all levels. On the other hand, due to non-consistent reference positions x_{ref} between the catchments the channel incision h_{inc}, vary considerably.

	(a) stream profile analysis statistics				(b) GIS zonal statistics	
level	$h_m \pm \sigma$ [m]	$h_{inc} \pm \sigma$ [m]	min-max [m]	h_Δ [m]	$h_m^{map} \pm \sigma$ [m]	min-max [m]
L0	**661**±46	62±40	566-732	-	665±20	581-709
L1	**765**±35	166±38	675-822	272	792±70	636-986
L2	**933**±48	306±107	854-1027	440	922±62	741-1140
L3	**1210**±40	306±107	1134-1268	717	1120±97	871-1469
L4	**1494**±56	792±196	1395-1550	1001	1579±187	1182-2318

Table 2: Global averaged statistics of all tributaries derived from stream power analysis is shown in (a) and derived zonal statistics from the DEM is given in (b). A comparison between (a) and (b) and therefore between two approaches shows reasonable correlation within the error bounds. The levels h_m are averaged altitudes of the palaeo-surfaces for all tributaries. The incision h_{inc} is calculated by averaging all level incisions from all tributaries but with varying reference points (see Table 1). The difference height h_Δ represents the relative height difference between the Gurk base level at Brückl and the remainder planation levels and are used for level correlation with the Styrian basin.

To identify palaeo-surfaces from channel profile analysis, modelled fits of equilibrium segments of most tributaries within the catchments of the major five drainages are extrapolated downstream. Only segments outside the glacially overprinted areas and only physically meaningful segments were included in the level clustering analysis. For example, physically meaningless extrapolation of segments under-run the main trunk profile. The elevation of palaeo-surfaces was then inferred from mean value statistics of the elevation of these extrapolated model profiles at an arbitrarily chosen reference point further downstream (for results see Table 1, 2a).

Independently of this analysis, field work and zonal statistics of the DEM (mean and variance value estimation of *z* values within polygonal zones) were used to confirm palaeo-surfaces and their characteristic deposits in the field (Table 2b). We started by field mapping with the younger, low level Pleistocene gravel terraces around the Althofen basin. The higher strongly incised strath terraces are more difficult to identify in the field. But together with a slope discrimination scheme (<15–20°) and knick-point analysis on the DEM, the inferred elevation of palaeo-surfaces could be considerably strengthened. Elevations in Table 2b are derived from this zonal statistics.

The geomorphological interpretation was performed on a DEM with 10 m cell size and Lambert Conformal Conical projection (MGI Austria Lambert) with 46° and 49° standard parallels (Cooperation OGD Austria, 2015).

The Matlab Toolbox of Schwanghart and Kuhn (2010) is used for channel data extraction from the DEM.

4. Results

The principal result of this study is the geomorphic map shown in Fig. 3. It shows the ice-free oasis of the Gurktal Alps surrounded by glaciers. The LGM glacial extent is based on van Husen (2011) but was modified according to some glacial imprints (or absence thereof) recognized on the DEM. Interpretation of these modified sections is supported by stream power analysis results as detailed below. Inside the ice-free region, the map shows knick-points (red asterisks) and k_{sn} values of major streams and tributaries. Importantly, the maps shows four palaeo-surfaces that are inferred from steepness analysis of the DEM and a subsequent clustering based on parentage to knick-points (see methods section). These inferred palaeo- surfaces are located at elevations that are below the Nockalm surface and above the Pleistocene terraces and will be interpreted as Late Miocene to Pleistocene base levels (palaeo-surfaces) in the discussion section.

The map also shows that the three major drainages of the Gurktal Alps (Metnitz, Gurk and Wimitz) have substantially different morphological characteristics (Fig. 5d, e, f, i). The northernmost (Metnitz) channel was within the region of the Pleistocene ice sheet and thus bears the morphological characteristics of a glaciated valley. However, the two major rivers of the ice-free region, the Gurk and the Wimitz, also have substantially different valley profiles: Although it was ice-free, the main part of the Gurk below the Glödnitz junction has a broad, flat, sediment covered valley floor (compare morphology in Fig. 1, 5d and geology in Fig. 2). Upstream of the Enge Gurk knick-point (Fig. 5a) the river has a morphologically complicated valley profile, which is known to be the consequence of spectacular river diversion and piracy processes in the glaciation periods, in particular in the vicinity of Prekowa Höhe (van Husen, 2012; Weiss, 1977). In contrast, the Wimitz (Fig. 5i) also lies outside the ice sheet but has a pronounced V-shaped valley with clearly step-shaped valley flanks at higher elevations indicating a different genesis. These apparent differences can be much better quantified, illustrated and interpreted by a careful analysis of their channel characteristics.

4.1 Channel analysis

The channel analysis shown in Figs. 6 and 7 shows for each of the major three rivers the channel profile (thick black line), catchment size and k_{sn} as a function of channel length, as well as the log(S) - log(A) plot used to derive k_{sn} and q for inferred equilibrium sections. These equilibrium sections (H) are colour coded according to their later interpretation in terms of the planation levels mapped on Fig. 3. These model curves (thin coloured lines on Figs. 6, 7) are extrapolated to lower elevations to infer uplift in the discussion section. Glaciated parts of the channel are shown between half brackets.

The Gurk channel profile contains several different sections with respect to both its glaciation and fluvial channel history (Fig. 6a). Upstream of the Enge Gurk, the channel reveals a strong non-equilibrium profile with several knick-points that spatially correlate with the known transitions from glacial to fluvial river segments (Fig. 6a). Most importantly, there is a 220 m high knick-point on-top of the step above Ebene Reichenau, below which the LGM frontier carved a U-shaped valley with clear glacial overprint. This step is also seen in all Gurk tributaries (Fig. 7a) that join the river above this knick-point, but also appears to correlate with some knick-points in Gurk tributaries downstream of Ebene Reichenau (e.g. weakly in Peiningbach and more pronounced at Görzbach, Fig. 7).

In the unglaciated Gurk section above the Ebene Reichenau knick-point, two equilibrium sections (H_1 = blue and H_2 = magenta) are interpreted from the slope - catchment data (inset Fig. 6a). Their downstream extrapolation levels out at roughly 1400 m and 1200 m, respectively. Both segments have high regression values for the concavity index ($\theta > 0.9$), indicating that they may not relate to strictly fluvial processes. In contrast, the k_{sn} values are different for the two segments: For the lower H_2 segment it is smaller by a factor two compared to the upper H_1 segment (Fig. 6a). Van Husen (2012) interpreted the H_2 segment as a lake sedimentation zone.

Below the Ebene Reichenau knick-point, two more equilibrium segments may be identified. H_3 lies largely in the glaciated section above the Enge Gurk upstream from Thörl, while H_4 lies within the Nock Mountains depression below the Enge Gurk where the river was entirely unglaciated. The concavity indices ($\theta_{H4} = 0.58$; $\theta_{H3} = 0.08$) indicate a fluvial regime for H_4 and the rather low value of H_3 is interpreted to be because of glacial overprint. Nevertheless, it will be shown below that the H_3 level aligns well with one of the mapped palaeo-surfaces inside the Nock Mountains depression. The 837 m high terrace at Albeck castle is the uppermost found occurrence of low terrace sediments in the Gurk valley (Fig. 3). Downstream of there, the Sirnitz junction to the Gurk is about 50–60 m deeply incised into low terrace and Würmian gravels.

Between these two inferred equilibrium sections H_3 and H_4 lies a 12 km long section of strong geomorphic disequilibrium, including the Enge Gurk and the section up to Prekowa Höhe. This section has very high k_{sn} and contains two separate steps. The upper step falls from a knick-point at Prekowa Höhe (~950 m) down to an intermediate level above Severgraben bridge. In this section, the Gurk is known to have experienced a history of forceful river bed displacement due to the glacial extent of the confluence between Mur and Drau glaciers in the Pleistocene (van Husen, 2012). Today, this section is observed by the unlikely course of the Gurk on the flanks of Scharriegel peak along which it is bound by a 50 m high wall of fluvial glacial sediments. The second step begins two kilometres past Severgraben bridge where the Gurk falls down from about 810 m along the Enge Gurk section to approximately 750 m inside the Nock Mountains

Figure 5: Field photographs of the Gurktal Alps. Locations are marked with red dots on Fig. 1. A: The river Gurk flowing on bedrock at the Enge Gurk location downstream of Severgraben bridge. Above the steep slope, the most prominent knick-point is located. B: Steep part of the Görzbach channel near Görzwinkel. C: Meandering section of the Leonhardsbach on the opposite side of the rim of the Nock Mountains depression. D: A panoramic view to the east of the middle Gurk section near Straßburg. At both valley fringes, remnant palaeo-surfaces of L_1, L_2 levels are visible. E: Eastward view of the glaciated Metnitz valley at Grades is shown with L_1, L_2 planation levels on the left hand side. Several stages of landscape evolution become visible with two U-stages on the top and finally a V-shape at the bottom of the cross-section. F: Southward view of the palaeo-surfaces L_2, L_3 levels from St. Florian church close to Gunzenberg. The surface is cut by a deeply incised Wimitz valley (left to right). G: Ground moraine in the Metnitz valley downstream of Metnitz is shown. H: The glacially overprinted Glödnitz valley. I: The upper Wimitz valley close to Goggau watershed. At the watershed, the valley is broad and rapidly narrows after 500 m in the downstream direction.

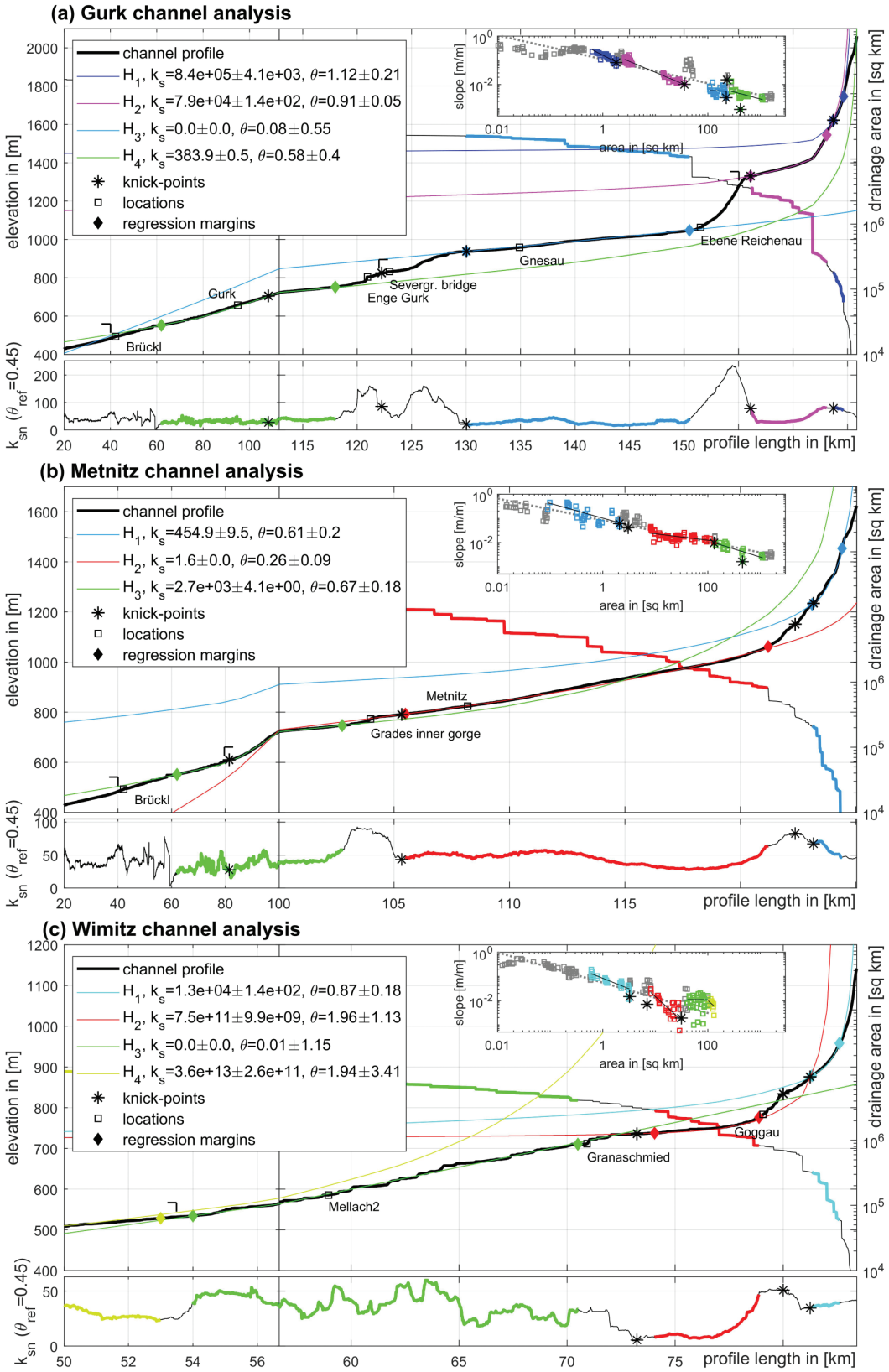

Figure 6: Channel profiles of the main river trunks of the Gurk, the Metnitz and the Wimitz. Note scale change in horizontal axes of all three plots. Below each channel profile, the k_{sn} values are shown. Pairs of equal colour diamond symbols are showing the regression interval, which also equals to coloured sections of the k_{sn} plot. The colour code of these equilibrium channel segments is also used in Figs. 3, 7 and 9. The thin coloured lines show the extrapolated modelled channel profiles for each segment. An asterisk symbol indicates a knick-point along the profile, squares are showing geographic locations and profile segments within a pair of brackets " ⌜"-"⌝ " are identifying glacially overprinted river sections. The small inset graph shows the log(*S*) – log(*A*) analysis together with the segment identification. In the Gurk profile a major knick-point is found close to Severgraben bridge, which separates the upper and the middle Gurk river valley. For the Metnitz a major knick-point is identified two kilometres east of the Metnitz village, which lies upstream of an inner gorge. For the Wimitz one major knick-point is found two kilometers southwest of Granaschmied, which is interpreted to mark the Pleistocene glacial frontier.

depression. The Enge Gurk gorge shows no glacial imprints at its side walls, which is interpreted to be the LGM transition margin (van Husen, 2012).

Tributaries to the Gurk main channel with equal stream order reveal some interesting changes when transiting the rim of the Nock Mountains depression. For example,

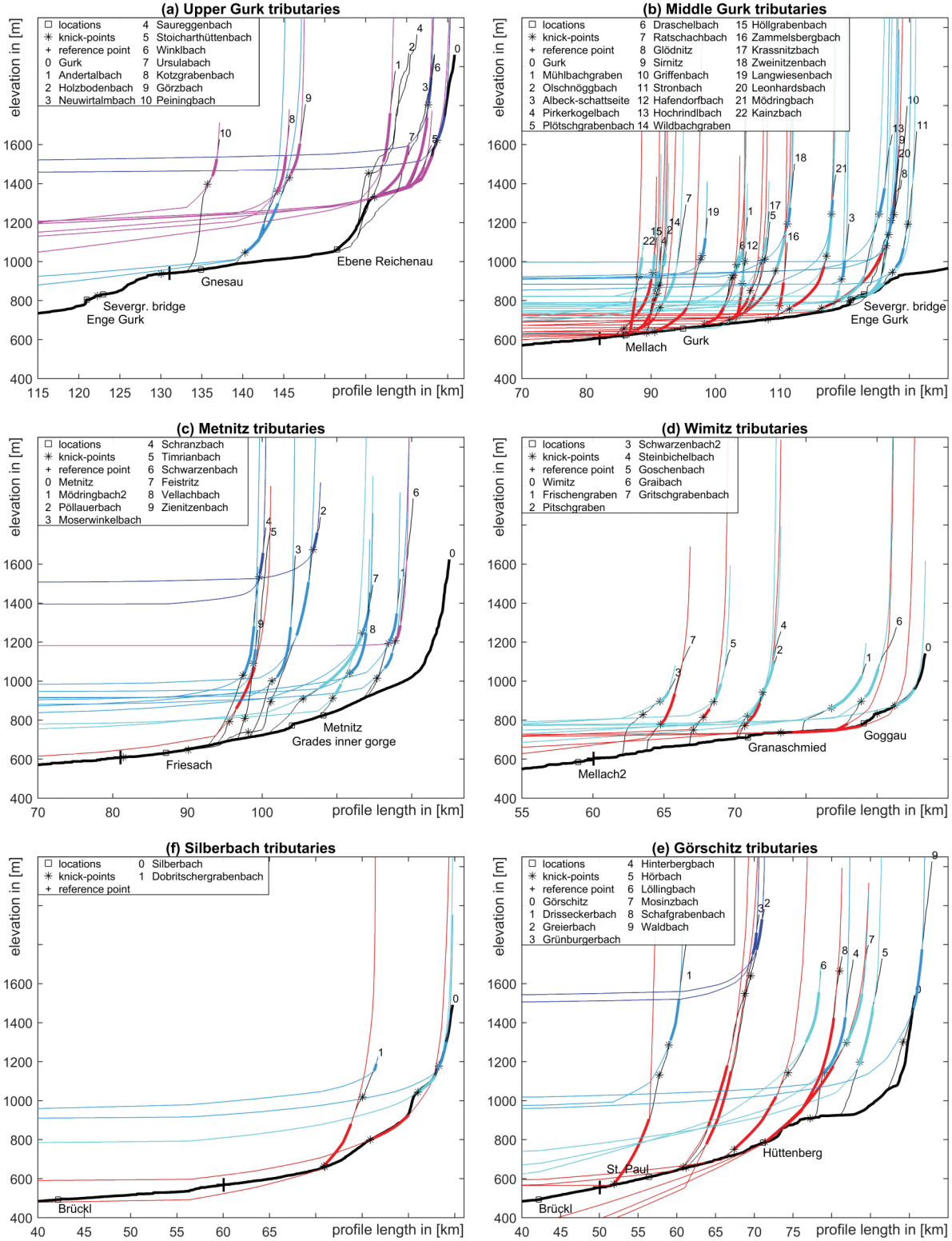

Figure 7: Channel profile analysis of tributaries to the upper Gurk, the middle Gurk, the Metnitz, the Wimitz, the Silberbach and the Görschitz rivers. Only tributaries with stable segments are displayed (compare river names with Fig. 3). Regression data was taken into account within the thick coloured intervals, while the model extrapolation is plotted by thin coloured lines. Downstream the extrapolations are indicating palaeo-surfaces showing a clustering tendency, which is indicated by colouring (L_0: red, L_1: cyan, L_2: light blue, L_3: magenta, L_4: blue). A "+" mark in the channel profile marks the arbitrarily chosen reference position x_{ref} where altitudes and incisions were taken for later on statistics (see Table 1 and Fig. 3). Clearly, an altitude correlation between tributaries can be observed.

the Görzbach in its middle section shows considerably steeper gradients than the Leonhardsbach inside the depression with its meandering characteristics (Fig. 5b, c). Therefore, (when excluding tributaries, that were affected by Pleistocene lake formation), k_{sn} values in the west outside the Nock Mountains depression are higher than inside the rim.

The Metnitz channel shows three equilibrium segments, all of which are subject to glacial overprint and are therefore probably not very meaningfully interpretable in terms of a fluvial incision model (Figs. 1b, 6b). The upper two of these segments, H_1 and H_2, have extremely low concavity indices ($\theta < 0.26$). H_1 is located in the head section of the valley where a steep swampy area is the source of the Metnitz, while H_2 covers the more gentle the valley floor, down to the entrance of the inner gorge near Grades. Extrapolation of the H_2 segment falls below today's topography, indicating that this section is over steepened, probably by glaciers in the Pleistocene. Glacial evidence along these segments is abundant, for example a ground moraine at about 21 km downstream of Metnitz (Fig. 5g) or a broad side moraine on the south side of the valley near Grades. A comparison of slopes of the northern and southern valley side in the vicinity of Metnitz reveals a difference in the spatial distribution of slope angle due to glacial overprint. The relict landscape on the southern side shows widespread flattened topography at top heights, while the glacially overprinted areas on the northern side have flush surfaces mostly at valley floors.

The lowest H_3 segment ($\theta = 0.67$), lies partially outside the glaciated regions and can also be found in fluvial regimes of the Gurk river area indicating that the glacial overprint here had only minor influence. The small transition zone between the segment H_1 and H_2 at profile length 104 km, aligns with the location of an inner gorge to the north of Grades. In accordance, the associated k_{sn} peak indicates high erosive resistance. Despite this, the k_{sn} plot reveals no further variations.

The Wimitz river has a steep, V-shaped inner gorge for much of its length between Granaschmied and Mellach. It has a grossly different appearance to the Gurk and Metnitz valleys, implying a different genesis. Within the Wimitz main trunk (Fig. 6c) four regression segments were found. H_4 is the lowest segment downstream of Mellach. It is affected by the Palaeo-Drau glacier and will not be discussed further.

Segment H_3 starts at Granaschmied just below the knick-point in the main valley and reaches downstream as far as the fluvioglacial terrace near Kraig (Vorstoß-schotter in Fig. 2) (Fig. 3). The elevation profile of this segment is largely linear. Accordingly, the catchment size hardly increases along this segment. The value $\theta = 0.01$ is below normal range for fluvial incision and has a large uncertainty. This section of the Wimitz valley constitutes the deeply incised V-valley with many hard-rock outcrops giving the profile segment a very rugged and unstable appearance. Wimitz tributaries in the H_3 segment have distinct knick-points some 100 vertical meters above the Wimitz main trunk at an elevation where the V-shaped inner gorge of the Wimitz flattens out into gentle slopes towards the flanking ridges of the Schneebauer and the Zammelsberg Ridge.

Above the Granaschmied knick-point the valley slope abruptly gets flattened up to Goggau. The regression estimate of H_2 is out of the plausible range for fluvial erosion. Therefore, a glacial overprint down to Granaschmied seems likely. Furthermore, the morphology of the valley (Fig. 5i) was interpreted as a glacial overridden water-shed, but due to missing surface textures in the DEM, these findings were disregarded in the geomorphological map and the LGM barrier was mapped west of Goggau.

Between the equilibrium segments H_1 and H_2 there is a knick-point on top of a steep step. Here the Wimitz leaves the broad main valley. The step is interpreted as a hanging valley, formed by the main glacier coming from the west. The k_{sn} between H_1 and H_2 shows an increase followed by a drop in the top section. This pattern is visible for many tributaries within the Nock Mountains depression.

4.2 Landforms

The strong disequilibrium observed in the channels is matched by a series of discrete shallow-slope segments on hill-slopes. Four of them are likely to be related to pre-Pleistocene processes and will form the focus of our discussion. In total, we recognize the following landforms in the Gurktal Alps: There are five types of sedimentary terraces that are discerned on the basis of their elevation, four types of strath terraces and/or palaeo-surfaces and two types of incised gorges (Fig. 3). Finally, there are alluvial plains and hill-slopes between different mapped surfaces that reflect incision periods between the two flanking landforms. These landforms are now described in a rough order from low to high and possibly from youngest to oldest.

The lowest landforms are the Holocene alluvial channels that are cut into the Würmian glacial terraces (dark green on Fig. 3). These channels are cut discretely into several terraces in the Althofen basin and in the Gurk valley between the Enge Gurk and the Glödnitz junction. However, below Glödnitz and above the Althofen basin, the Holocene Gurk appears to have different characteristics. The channel still lies below the Würmian terrace remains, but it meanders on an alluvial plain, indicating that it may be aggrading, rather than incising.

The mapped terraces include two low terraces that are both considered to have formed during the Würmian glaciation period (GeoServices-KAGIS, 2017; Thiedig et al., 1999). They lie at elevations of 10 m and 30 m above the current river (light and dark yellow on Fig. 3). We also mapped some glacial terraces in the Gurk valley above Prekowa Höhe and in the Metnitz valley above Metnitz of which we do not know the age and which are therefore separately mapped but may also be Würmian (brown on Fig. 3).

The highest mapped terrace is here termed L_0 (red on Fig. 3). In the Gurktal Alps, this terrace forms several prominent outcrops between Gurk and Wimitz, southwest of Althofen at an elevation of 665 m (Table 2b). It is reported to be of Rissian age at least (GeoServices-KAGIS, 2017; Thiedig et al., 1999). This elevation is matched by a level that is not seen as a shallow relief surface in the landscape, but—considering the upstream location of the reference point—it is evident in the channel profiles of a series of tributaries in the middle Gurk (altitude 616–731 m) and Wimitz (672–732 m) (see Table 1, Fig. 7). It is possibly also seen in a single tributary of the Metnitz. Because of the good correlation of the Rissian terrace and the channel analysis for L_0, this level is inferred to be Rissian across the Gurktal Alps and lower landforms that are incised up to the order of 200 metres below this level are inferred to be younger. This is particularly important for the Wimitz where we interpret small terraces between Kraig and Mellach to belong to the L_0 level. No lower/younger terraces are found in the Wimitz itself.

The V-shaped deep gorge of the Wimitz is mapped as a landform of its own, because of its distinct appearance. It forms an actively incising bedrock channel that appears to have cut into the much flatter L_0 level by some 200 meters. A similar V-shaped but less pronounced gorge was found in the Feistritz and Vellachbach valley that drain into the Metnitz from the south near Grades (Fig. 3). To the north of Grades the Metnitz shows a ca. 500 m long deep gorge. Because of missing glacial imprints this section is classified as an inner gorge in the sense of Montgomery and Korup (2010), that is interpreted to be formed by fluvial processes despite being overlain by glaciers.

Palaeo-surface L_1 (cyan on Fig. 3; 792 ± 70 m Table 2b) is the lowest recognized strath terrace in the Gurktal region that is seen both as low-slope surfaces in the landscape (792 ± 70 m) and as discrete equilibrium segments in channels with an elevation of 765 ± 35 m (Table 2a, b). Many tributaries in all analysed catchments show stable segments of this level. For the Wimitz this level separates clearly from the L_0 level in altitude. In the middle Gurk valley, the separation between L_0 and L_1 becomes clear due to the equilibrium segment succession along the tributary profiles. However, a clear distinction of the two levels in the field or by DEM analysis is less clear. One reason can be addressed to a north-west trending fault mapped at Gurk village (Fig. 3 with fault data from Geological Survey of Austria (2017)). The altitudes of the L_1 level appears to be offset by about 100–150 m across the fault stepping down in north-east direction indicating post-L_1 level, probably Pleistocene, activity. In the geomorphological map, the biggest fraction of this L_1 relict surface is grouped at the margin from west to north-west around the high terrace in the Althofen basin. Smaller and more fractured L_1 remnants can be found in the downstream part of the middle Gurk valley, but no surface is preserved in the Wimitz valley.

Palaeo-surface L_2 (light blue on Fig. 3; 922 ± 62 m Table 2b) is widespread across the Metnitz and the middle Gurk catchments (Fig. 5d). No related regression segments are found for the channel profiles along the course of the Wimitz valley. There is one knick-point at the head of the Goschenbach (see Fig. 3). Another one at the Rabingbach, which is a tributary of the lower Gurk and one knick-point at the Bacherngrabenbach, which drains into the Glan. In between, most knick-points have probably already reached the channel head. Also the middle Gurk river exhibits large areas of this level at its northern margin. Interestingly, the L_2 level aligns well with the elevation of the knick-point near Urschlerwirt in the Gurk channel (Fig. 6, 7), indicating a wide distribution of palaeo-surface L_2 downstream of the knick-point and inside the Nock Mountains depression.

Palaeo-surface L_3 (magenta on Fig. 3; 1120 ± 97 m Table 2b) is the most widespread strath terrace in the Nock Mountains depression. It occupies large areas on top of the Mödring and the Wimitz Mountains (Fig. 3, 5f). Only small remnants of this palaeo-surface are identified in the Görzbach and Kotzgraben valley in the upper Gurk river region. Conversely, stable river segments of this level are almost absent inside the Nock Mountains depression, but common in the upper Gurk river region (Fig. 7). Only a single short channel segment, namely the Schwarzenbach on the northern flank of the Metnitz valley at Mt. Hirschstein, shows evidence for the L_3 segment in a river channel. Its regression results in a rather high and unconfident $\theta = 1.97 \pm 0.52$ value compared to theta values between 0.48 and 0.91 with confidence intervals ranging from ± 0.03 to ± 0.12 in the upper Gurk region.

Palaeo-surface L_4 (blue on Fig. 3; 1579 ± 187 m on Table 2b) is the highest strath terrace mapped here. Because of its high elevation, it is only seen in the high-lying regions outside the rim of the Nock Mountains depression and at top ridges of the Mödring Mountains. In particular, it is present to the north-east of the Gurk river region, between the Scharriegel and the Eisenhut peaks. The L_4 segments of the Metnitz and the upper Gurk cluster around 1450–1500 m, while related levels in the Görschitz catchments at the slopes of the Saualpe reach heights of 1531 m (Table 1).

Low slopes and smooth surface textures (Fig. 3) indicate the existence of further palaeo-surfaces at higher altitudes on top of the nunataks north of the investigated region, for example on top of Grebenzen peak. Widespread palaeo-surfaces are also visible on the southern slopes of the Metnitz Mountains toward Murau. These regions are a likely to be an eastward extension of the Nockalm surface, located north-west from the studied region. However, as they lie clearly within the region glaciated in the Pleistocene their origin remains enigmatic without detailed morphological analysis and we will not discuss them in further detail here.

5. Discussion

In the analysis presented above there is no tight relationship between the elevations inferred from the equilibrium

segments of channels, H (channel analysis section, Figs. 6, 7 and Table 1, 2a) and the elevation of the related relict surface, L (Fig. 3, Table 2b). This is partly due to the upstream travel of the knick-points, which highly depends on travel time and the amount of discharge (Fig. 4). Furthermore, it is questionable whether the chosen segments upstream of the transition knick-point can be regarded as an equilibrium segment as illustrated in the schematic geomorphological evolution model in Fig. 4. Nevertheless, the planation levels and extrapolated equilibrium segments channel profiles correlate within error so that they can be attributed to the same landscape-forming processes. This is emphasized by using the same colour coding in Fig. 6 for the main trunks and Fig. 7 for tributary channels (only fluvial channels with stable segments are shown) as for the palaeo-surfaces on Fig. 3.

On the basis of this correlation it is now possible to infer amounts of fluvial incision following each landform in the Gurktal Alps. Table 1 shows that the elevation h_m for a given inferred level is very similar for all considered catchments. This is confirmed by the small errors that arise when the elevation h_m is averaged over all catchments (Table 2). However, the inferred amount of incision varies more dramatically between catchments, which is also related to the local selection of the reference point. In particular, for level L_0 the incision of the Wimitz channel is substantially higher than in all other catchment (Table 1).

The exceptional amount of post-L_0 level incision of the Wimitz allows the interpretation of the origin of this gorge. Its incision is consistent with the field mapping that identified the deep gorge of the Wimitz valley as its own landform (Fig. 3). As discussed above, the Wimitz valley has a very rugged unstable appearance. It seems possible that this observed profile instability is caused by mass movements from the side-walls during heavy incision periods, which are still not equilibrated (moved upward). In view of presence of Rissian terraces at the L_0 level we suggest that this incision occurred since the Late Pleistocene and is thus related to fluvial processes during the glaciation periods. This interpretation is supported by the Wimitz tributaries. Almost all Wimitz tributaries confluence with the main trunk forming a non-glacial hanging valley. We suggest that this is because strong fluvial erosion eroded the Wimitz when the Gurk drained via the Wimitz valley during the glaciation periods.

Although the Gurk valley has very different morphological characteristics, we suggest here that its morphology may be interpreted in terms of a related process. The pre-Würmian channel may have been very similar to that of the Wimitz today and was filled by sediments in the aggregating section between Glödnitz and the Althofen basin during the Holocene. The pre-Würmian channel in this part of the Gurk valley may lie some hundreds of meters at depth and had a pre-Würmian appearance similar to that of the Wimitz valley today. This interpretation is supported by the lower part of channels profiles of several Gurk tributaries (Fig. 7). In those, the lowest knick-points are located some 5–20 m below the surrounding low terrace. This can be observed most prominently at, for example, the Sirnitz, Hochrindlbach, Griffenbach, Mödringbach and tributaries further downstream to Mellach (red asterisks in Fig. 3). These knick-points are related to the L_0 level, which is interpreted to represent the base level in the Rissian (see below).

The interpretation of the Gurk channel is supported by a topographic analysis (Fig. 8). The slope map (Fig. 8b) shows steep homogeneous slopes at the southward orientated flank at the Knittel, Scharriegel and the Applitschberg (see also Fig. 3). This contour margin is interpreted to be the transition line between the glacial carving (LGM frontier) and a palaeo-surface, which extends to the north. This is also supported by van Husen (2012) who noted that the Gurk channel bed in this section might be formed sub-glacial.

The mapped strath terraces L_1–L_4 are all substantially higher and are likely to be much older. They lie outside the parts of the Eastern Alps that were glaciated in the last two million years and are thus likely to reflect pre-Pleistocene relict surfaces that can be interpreted in terms of discrete steps in the surface uplift history of the range. In order to interpret this on the scale of the Eastern Alps, it is important to correlate these surfaces with other palaeo-surfaces in the non-glaciated parts of the Eastern Alps.

5.1 Correlation of the palaeo-surfaces with other regions

Palaeo-surfaces similar to those mapped here have been mapped in the Nock Mountains region (Hejl, 1997, 1998), the Grazer Bergland (Winkler Hermaden, 1955, 1957; Wagner et al., 2010), the Niedere Tauern (Dertnig et al., 2017), the Koralpe and Pohorje Massifs (Legrain et al., 2014), the Northern Calcareous Alps in general (Frisch et al., 2001) and the Transdanubian Range (Ruszkiczay-Rüdiger et al., 2011, 2018). However, if it is the aim to infer aspects of the uplift history of the range, it is circular to correlate palaeo-surfaces of corresponding elevation with corresponding genesis or age and other criteria must be found.

For example, within the investigated region, extrapolated channel profiles in the Görschitz valley show four discrete levels—akin to the remainder of the Gurktal region. However, the highest level L_4 appears to be discretely higher than in the Gurktal region and the lowest level L_0 seems to be in disequilibrium (Fig. 7e). This might be interpreted as a proxy for activity of the Görschitztal fault before L_3 was uplifted and also for the recent L_0 level which still appears out of equilibrium. Furthermore, k_{sn} within the Nock Mountains depression is below 100 for all catchments, except the western slope of the Saualpe where values above k_{sn} 200 are reached, indicating a younger uplift impulse there. Therefore, the Görschitztal fault (Fig. 3) is suggested to be still active.

Corresponding problems persist in correlations with other regions. The Gurktal Alps are separated from the well-known planation levels in the Styrian Block by at

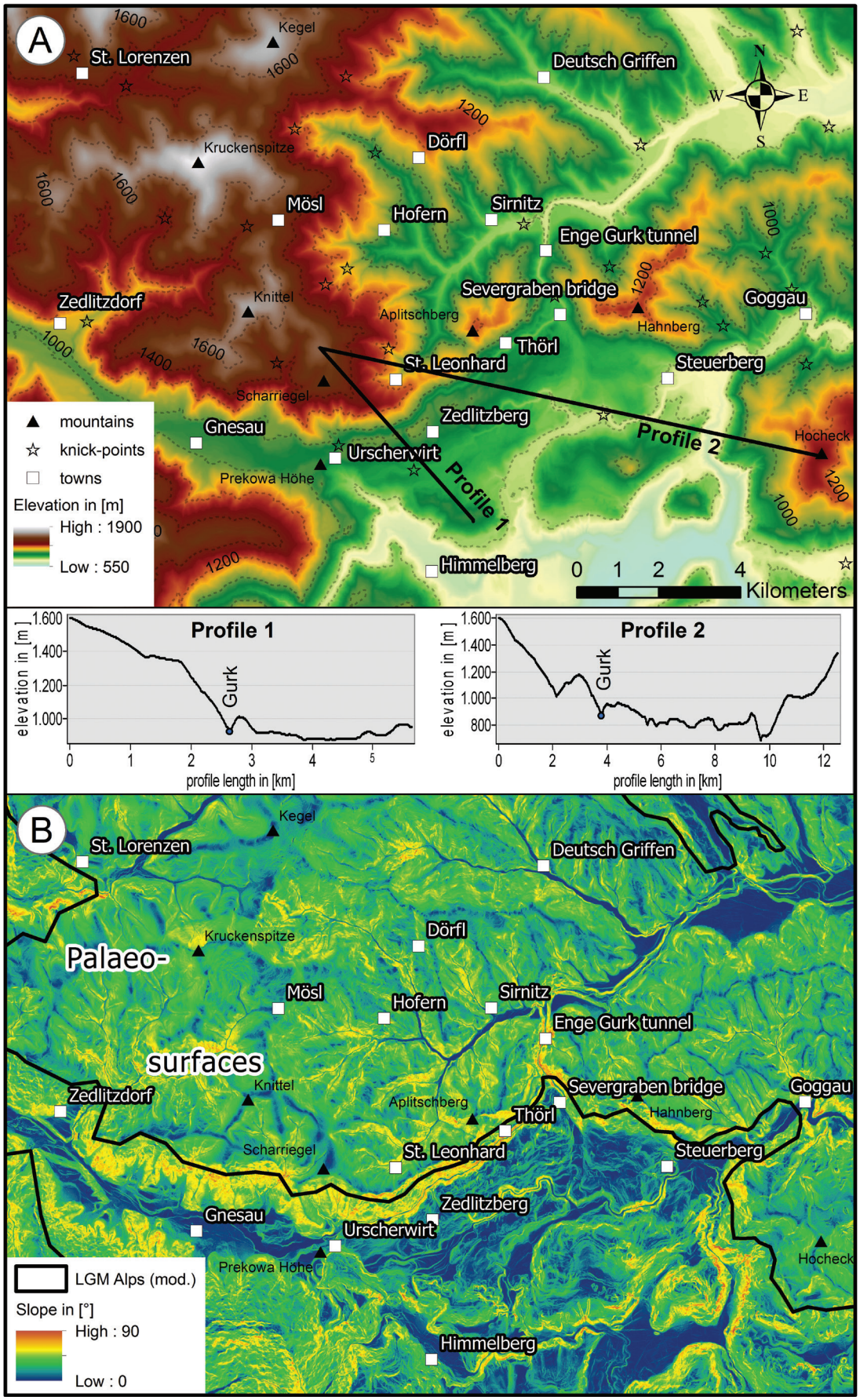

Figure 8: Morphological maps of the transition area between upper and lower Gurk valley around Prekowa Höhe. A: Digital elevation model (Cooperation OGD Austria, 2015) with two profiles along the rim of the Nock Mountains depression, which highlight the instability of the Gurk channel in this region. B: Slope map of the upper Gurk valley, which emphasizes paleo-Gurk channel locations and which identifies a palaeo-surface to the northeast.

least two active fault systems, namely the Pöls-Lavanttal and the Görschitztal fault system. Conversely, relative to the planation levels of the Northern Calcareous Alps, the Gurktal Alps are separated by the Ennstal fault, although Dertnig et al. (2017) have shown that planation levels of inferred same age across the Ennstal fault are at the same elevations. Nevertheless, due to unknown amounts of differential uplift between different regions we perform the correlation below not with respect to absolute elevation but relative to the base level in the main channel (Fig. 9).

A correlation with the well-known planation levels in the Styrian Block is shown in Fig. 9a. There, the elevations for pre-Pleistocene palaeo-surfaces as documented by Wagner et al. (2011) are shown relative to the local level of the Mur river. They are shown in comparison to the planation levels documented here. These are shown relative to the base level of the Gurk channel in Brückl at 493 m altitude, which is located at the lowest possible level outside the palaeo-glaciation and still western of the active Görschitztal fault. It may be seen that the L_1 level documented here correlates well with the Styrian Stadelberg/Zahrerberg level (Pliocene/Pleistocene according to Wagner et al. (2011)). The L_2 level correlates with the Early to Late Pliocene Hochstraden level. Given the closer proximity of the Gurktal region to the higher main axis of the Alps, we suggest that the widespread L_3 level correlates with the Early Pliocene Trahütten level and the L_4 level as mapped here with the Late Miocene to Early Pliocene Hubenhalt level of the Styrian Block. The bandwidth of the Gurktal palaeo-surfaces altitudes in Wagner et al. (2011) are interpreted as extreme values (minimum or maximum), while min-max ranges, mean values and 1σ intervals are given for the Gurktal surfaces.

In other regions, the known planation levels are even higher and thus above the maximum elevation of the Gurktal Alps. For example, the Nockalm surface at an elevation of 1700–2200 m is higher than the L_4 level as mapped here and thus probably of older age. It possibly correlates with some levels observed at Mt. Grebenezen north of the Metnitz valley. In the Niedere Tauern region, Dertnig et al. (2017) mapped three palaeo-surface levels with the lowest being located at about 1600 m. This level may relate to the L_4 level documented here. Interestingly, this level also corresponds in elevation to the so called Giant cave level in the Northern Calcareous Alps which has also been inferred to be of Latest Miocene or Pliocene age (Dertnig et al., 2017).

5.2 Age of the surfaces and timing of uplift

Although little is known about the absolute age of the palaeo-surfaces in the Gurktal Alps, the inferred correlation with other regions can be used to suggest an uplift history for the region (Fig. 9b). This uplift history is constructed using the ages of the palaeo-surfaces in the Styrian Block and the elevations and amounts of incision as documented here for the corresponding levels in the Gurktal Alps. The uplift curve and uplift rates shown in Figure 9b are interpreted as a temporally blurred lower limit, because the interpolation between planation stages is assumed to be linear, ignoring periods or quiescence that must have formed the Piedmont-step landscape (Spreitzer, 1932). The analysis suggests that at least some 1000 m of uplift and incision occurred in the last six million years. The analysis suggests an accelerated uplift in the time from 3.0–4.5 Ma with a peak uplift rate around 0.35 mm/a at 4 Ma (Early Pliocene).

Interestingly, this interpretation is nicely consistent with Hejl (1997, 1998) who inferred a final stage of cooling related to rock uplift and erosion following a Late Miocene period of stasis from low-temperature geochronological data, which they suggest correlates with the build-up

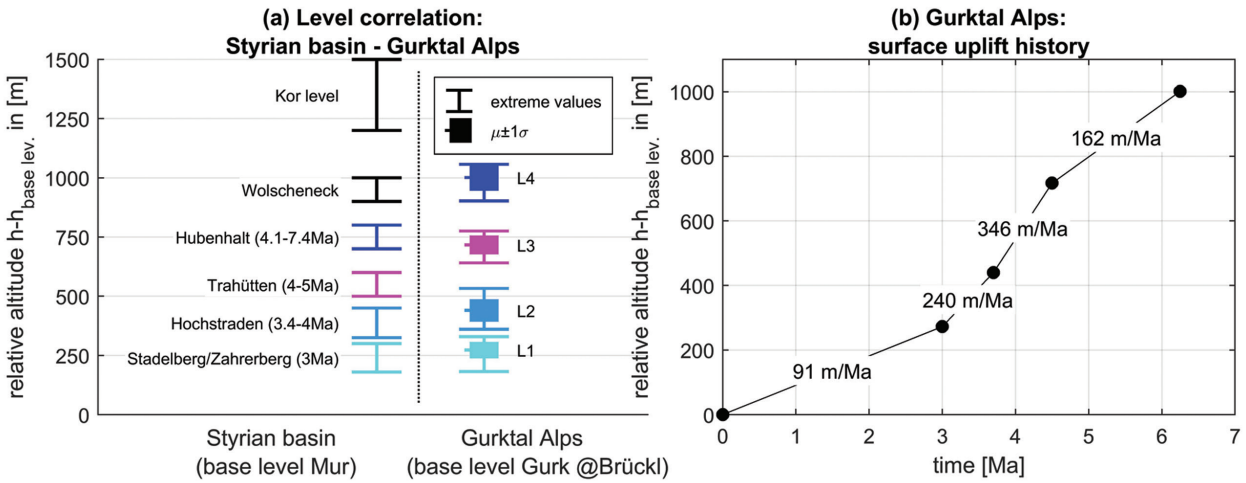

Figure 9: A: Comparison of the elevation of palaeo-surfaces L_1–L_4 as mapped here (elevation is shown above the Gurk river level in Brückl at 493 m) with known palaeo-surfaces in the ranges surrounding the Styrian basin (according to Wagner et al. (2011) with elevation measured relative above Mur river level). Note that within error there is good correlation. In general, the Gurktal region shows higher relative altitudes for older terraces. B: Based on age constraints from the Styrian basin a lower boundary for uplift is estimated, assuming negligible denudation of the relict landscape levels L_1–L_4. Based on this model major parts of the topography were uplifted within the last 6 Ma with a strong peak in uplift between 3–4.5 Ma.

of the Nockalm planation surface. As such, the Nockalm surface is likely to be only somewhat older than 7 Ma (Fig. 9). In particular, Hejl (1997, 1998) suggests strong steady denudation starting from four million years ago until today. Reinecker (2000), on the other hand inferred more gentle, continuous exhumation spread over several phases within an extended time range since the Late Miocene. To the south of the Wörthersee, Neubauer et al. (2018) documented a Late Miocene to Pliocene exhumation phase.

Our interpretation is also consistent with Wagner et al. (2010) who revealed about 500 m incision of the Mur river during the last four million years within the Palaeozoic of Graz. Wagner et al. (2010) also documented a decrease of incision rate of the Mur river in the last two million years. While they did not determine if this decrease in incision is related to a decrease in uplift rate or due to transient aggregation periods of the river in the Pleistocene, we note that it is paralleled by our analysis for the Gurktal Alps, which shows a considerably slow-down of uplift to 0.1 mm/a since 3 Ma and to 0.16 mm/a past 4.5 Ma

Correlation with our data for the Pleistocene can also be found for the Danube river in the Pannonian basin. Ruszkiczay-Rüdiger et al. (2011, 2018) reports ^{10}Be derived denudation rates around 3.5–20 m/Ma of terraces in the Transdanubian Range. Also, Šujan et al. (2017) inferred an upper bound of uplift rate of 26 m/Ma from ^{26}Al/^{10}Be burial age dating in the Stará Garda Cave in the Malé Karpaty Mts. (Western Carpathians) in western Slovakia.

6. Conclusion

Channel analysis and mapping in the Gurktal Alps reveals a series of geomorphic disequilibrium features like knick-points in most tributaries to the main drainages of the Gurktal Alps: the Gurk, Metnitz, Wimitz, Silberbach and Görschitz rivers. The disequilibrium features in the channels correlate with low relief surfaces mapped in the field. In total we recognize five types of glacial terraces, two types of gorges and four levels of palaeo-surfaces that lie at roughly 800 m (level L_1), 900 m (level L_2), 1200 m (level L_3) and 1500 m (level L_4) surface elevation. These four levels are all below the well-known Nockalm surface (1700–2200 m elevation) and document a stair-shaped landscape that descends from the Nockalm region towards the Klagenfurt basin. Interpretation and correlation of these levels between the different catchments of the Gurktal Alps and across other regions of the Eastern Alps that escaped Pleistocene glacial reshaping reveals the following:

- Correlation of the mapped levels with well-known palaeo-surfaces further east suggests that L_1 level correlates with the Styrian Stadelberg/Zahrerberg level, L_2 level with the Hochstraden level, L_3 level with the Trahütten level and L_4 with the Hubenhalt level of the Styrian Block. The correlation suggests that there are about 1000 m of surface uplift and incision in the last 6 Million years in the Gurktal Alps.
- The inferred uplift history appears to have accelerated around 4 Ma. This interpretation is consistent with Hejl (1997, 1998) who recognize a final stage of cooling following a late Miocene phase of stasis from low-temperature geochronology.
- A good correlation of knick-points in tributaries to the Wimitz with a Rissian terrace level suggests that the V-shaped channel of the Wimitz is no older than Rissian glaciation period. We suggest that the entire Gurk catchment drained through the Wimitz valley from the Pleistocene to the pre-Würm (LGM) and carved the V-shaped deep gorge in a relatively short period. Conversely, the Gurk channel may have altered to its present state starting from the LGM and was only then filled in by Würmian and Holocene alluvial sediments.
- Evidence for offset of the Rissian planation surface across the Görschitz valley suggests that the Görschitz fault is still active today. This interpretation is also supported by some model fits for channels in the Saualpe and, high k_{sn} values.

Acknowledgements

The authors are grateful to J. Schlammberger from the Amt der Kärntner Landesregierung, for providing the shape-file of the 1:200.000 geology from the Kärnten Atlas portal (GeoServices-KAGIS, 2017). This data was very helpful due to the scarcity of available resources for this region. Furthermore, we wish to thank our reviewers L. Fodor and C. Grützner for their comments and suggestions, which helped to improve this manuscript.

References

Aigner, A., 1922. Geomorphologische Beobachtungen in den Gurktaler Alpen. Sitzungsberichte der mathematisch-naturwissenschaftlichen Klasse, Akademie der Wissenschaften, Wien, 131, 243–278.

Aigner, A., 1924. Über tertiäre und diluviale Ablagerungen am Südfuße der Niederen Tauern. Jahrbuch Geologische Bundesanstalt, Wien, 74, 179–196.

Baran, R., Friedrich, A.M., Schlunegger, F., 2014. The late Miocene to Holocene erosion pattern of the Alpine foreland basin reflects Eurasian slab unloading beneath the western Alps rather than global climate change. Lithosphere, 6/2, 124–131. https://doi.org/10.1130/L307.1

Bartosch, T., Stüwe, K., Robl, J., 2017. Topographic evolution of the Eastern Alps: The influence of strike-slip faulting activity. Lithosphere, 9/3, 384–398. https://doi.org/10.1130/L594.1

Cooperation OGD Austria, 2015. Digitales 10m—Geländemodell aus Airborne Laserscan Daten. http://gis.ktn.gv.at/OGD/Geographie_Planung/ogd-10m-at.zip

Dertnig, F., Stüwe, K., Woodhead, J., Stuart, F.M., Spötl, C., 2017. Constraints on the Miocene landscape evolution of the Eastern Alps from the Kalkspitze region, Niedere

Tauern (Austria). Geomorphology, 299, 24–38. https://doi.org/10.1016/j.geomorph.2017.09.024

Dixon, J.L., von Blanckenburg, F., Stüwe, K., Christl, M., 2016. Glaciation's topographic control on Holocene erosion at the eastern edge of the Alps. Earth Surface Dynamics, 4/4, 895–909. https://doi.org/10.5194/esurf-4-895-2016

Ebner, F., Sachsenhofer, R.F., 1995. Palaeogeography, subsidence and thermal history of the Neogene Styrian Basin (Pannonian basin system, Austria). Tectonophysics, 242/1-2, 133–150. https://doi.org/10.1016/0040-1951(94)00155-3

Exner, C., 1949. Beitrag zur Kenntnis der jungen Hebung der östlichen Hohen Tauern. Mitteilungen der Geographischen Gesellschaft Wien, 91, 186–196.

Exner, C., 1989. Geologie des mittleren Lungaus. Jahrbuch Geologische Bundesanstalt, Wien, 132/1, 7–103.

Exner, C., Hejl, E., Mandl, G.W., 2005. Geologische Karte der Republik Österreich: 157-Tamsweg. Geologische Bundesanstalt, Wien, ÖK 1:50.000.

Frisch, W., Kuhlemann, J., Dunkl, I., 2001. The Dachstein paleosurface and the Augenstein Formation in the Northern Calcareous Alps—a mosaic stone in the geomorphological evolution of the Eastern Alps. International Journal of Earth Sciences, 90/3, 500–518. https://doi.org/10.1007/s005310000189

Frisch, W., Kuhlemann, J., Dunkl, I., Brügel, A., 1998. Palinspastic reconstruction and topographic evolution of the Eastern Alps during late Tertiary tectonic extrusion. Tectonophysics, 297/1, 1–15, https://doi.org/10.1016/S0040-1951(98)00160-7

Genser, J., Cloetingh, S.A., Neubauer, F., 2007. Late orogenic rebound and oblique Alpine convergence: New constraints from subsidence analysis of the Austrian Molasse basin. Global and Planetary Change, 58/1-4, 214–223. https://doi.org/10.1016/j.gloplacha.2007.03.010

Geological Survey of Austria, 2017. ArcGIS Map Service: Geologic structure layer of projekte_onegeology / 1GE_GBA_500k_Surface_Geology, http://gisgba.geologie.ac.at/arcgis/services

GeoServices-KAGIS, 2017. ArcGIS shapefiles of geological map 1:200.000 of Carinthia—Kärnten Atlas V4. Amt der Kärntner Landesregierung. https://gis.ktn.gv.at

Hack, J., 1957. Studies of longitudinal profiles in Virginia and Maryland. U. S. Geological Survey, Professional Paper 294-B. https://doi.org/10.3133/pp294B

Hejl, E., 1997. 'Cold spots' during the Cenozoic evolution of the Eastern Alps: thermochronological interpretation of apatite fission-track data. Tectonophysics, 272/2–4, 159–173.https://doi.org/10.1016/S0040-1951(96)00256-9

Hejl, E., 1998. Über die känozoische Abkühlung und Denudation der Zentralalpen Östlich der Hohen Tauern – eine Apatit-Spaltspuranalyse. Mitteilungen der Österreichischen Geologischen Gesellschaft, 89, 179–199.

Hergarten, S., Robl, J., Stüwe, K., 2016. Tectonic geomorphology at small catchment sizes—extensions of the stream-power approach and the chi method. Earth Surface Dynamics, 4, 1–9. https://doi.org/10.5194/esurf-4-1-2016

Howard, A.D., Kerby, G., 1983. Channel changes in badlands. Geological Society of America Bulletin, 94, 739–752. https://doi.org/10.1130/0016-7606(1983)94<739:CCIB>2.0.CO;2

van Husen, D., 1987. Die Ostalpen in den Eiszeiten. Geologische Bundesanstalt, Wien.

van Husen, D., 2011. Quaternary glaciations in Austria. Developments in Quarternary Sciences, Elsevier, 15, 15–28. https://doi.org/10.1016/B978-0-444-53447-7.00002-7

van Husen, D., 2012. Zur glazialen Entwicklung des oberen Gurktales. Jahrbuch Geologische Bundesanstalt, Wien, 152/1–4, 39–56.

Kirby, E., Whipple, K.X., Tang, W., Chen, Z., 2003. Distribution of active rock uplift along the eastern margin of the Tibetan Plateau: Inferences from bedrock channel longitudinal profiles. Journal of Geophysical Research, 108/B4. https://doi.org/10.1029/2001JB000861

Kuhlemann, J., Dunkl, I., Brügel, A., Spiegel, C., Frisch, W., 2006. From source terrains of the Eastern Alps to the Molasse Basin: Detrital record of non-steady-state exhumation. Tectonophysics, 413/3–4, 301–316. https://doi.org/10.1016/j.tecto.2005.11.007

Kuhlemann, J., Kempf, O., 2002. Post-Eocene evolution of the North Alpine Foreland Basin and its response to Alpine tectonics. Sedimentary Geology, 152/1–2, 45–78. https://doi.org/10.1016/S0037-0738(01)00285-8

Legrain, N., Stüwe, K., Wölfer, A,. 2014. Incised relict landscapes in the eastern Alps. Geomorphology, 221, 124–138. https://doi.org/10.1016/j.geomorph.2014.06.010

Montgomery, D.R., Korup, O., 2010. Preservation of inner gorges through repeated Alpine glaciations. Nature Geoscience, 4, 62–67. https://doi.org/10.1038/ngeo1030

Neubauer, F., Pistotnik, J., 1984. Das Altpaläozoikum und Unterkarbon des Gurktaler Deckensystems (Ostalpen) und ihre paläogeographischen Beziehungen. Geologische Rundschau, 73/1, 149–174.

Neubauer, F., Heberer, B., Dunkl, I., Liu, X., Bernroider, M., Dong, Y, 2018. The Oligocene Reifnitz tonalite (Austria) and its host rocks: implications for Cretaceous and Oligocene—Neogene tectonics of the southeastern Eastern Alps. Geologica Carpathica, 69/3, 237–253. https://doi.org/10.1515/geoca-2018-0014

Neumann, H.H., 1989. Die Oberkreide des Krappfeldes. Arbeitstagung Geologische Bundesanstalt, Wien, 70–79.

Perron, J.T., Royden, L., 2013. An integral approach to bedrock river profile analysis. Earth Surface Processes and Landforms, 38/6, 570–576. https://doi.org/10.1002/esp.3302

Rantitsch, G., Russegger, B., 2000. Thrust-related very low grade metamorphism within the Gurktal Nappe Complex (Eastern Alps). Jahrbuch Geologische Bundesanstalt, Wien 142/2, 219–225.

Ratschbacher, L., Frisch, W., Linzer, H.G., 1991. Lateral extrusion in the Eastern Alps, part 2: Structural analysis. Tectonics, 10/2, 257–271. https://doi.org/10.1029/90TC02623

Reinecker, J., 2000. Stress and deformation: Miocene to present-day tectonics in the Eastern Alps. Tübinger Geowissenschafliche Arbeiten, Reihe A, 55.

Royden, L., Perron, J.T., 2013. Solutions of the stream power equation and application to the evolution of river longitudinal profiles. Journal of Geophysical Research: Earth Surface, 118, 497–518. https://doi.org/10.1002/jgrf.20031

Ruszkiczay-Rüdiger, Zs., Braucher, R., Csillag, G., Fodor, L.I., Dunai, T.J., Bada, G., Bourlés, D., Müller, P., 2011. Dating Pleistocene aeolian landforms in Hungary, Central Europe, using in situ produced cosmogenic ^{10}BE. Quaternary Geochronology, 6/6, 515–529. https://doi.org/10.1016/j.quageo.2011.06.001

Ruszkiczay-Rüdiger, Zs., Csillag, G., Fodor, L., Braucher, R., Novothny, Á., Thamó-Bozsó, E., Virág, A., Pazonyi, R., Timár, G., and ASTER Team, 2018. Integration of new and revised chronological data to constrain the terrace evolution of the Danube River (Gerecse Hills, Pannonian Basin). Quaternary Geochronology, 48, 148–170. https://doi.org/10.1016/j.quageo.2018.08.003

Schwanghart, W., Kuhn, N.J., 2010. Topotoolbox: A set of Matlab functions for topographic analysis. Environmental Modelling & Software, 25/6, 770–781. https://doi.org/10.1016/j.envsoft.2009.12.002

Spiegel, C., Kuhlemann, J., Dunkl, I., Frisch, W., 2001. Paleogeography and catchment evolution in a mobile orogenic belt: the Central Alps in Oligo–Miocene times. Tectonophysics, 341/1–5, 33–47. https://doi.org/10.1016/S0040-1951(01)00187-1

Spreitzer, H., 1932. Zum Problem der Piedmonttreppe. Mitteilungen der Geographischen Gesellschaft Wien, 75, 327–364.

Šujan, M., Lačný, A., Braucher, R. Magdolen, P., and ASTER Team, 2017. Eearly Pleistocene age of fluvial sediments in the Stará Garda cave revealed by ^{26}Al/^{10}Be burial dating: implications for geomorphic evolution of the Male Karpaty Mts. (western Carpathians). Acta Carsologica, 46/2–3, 251–264. https://doi.org/10.3986/ac.v46i2-3.5157

Thiedig, F., van Husen, D., Pistotnik, J., 1999. Geological map of Austria 1:50,000, GK sheet 186 Sankt Veit an der Glan. Geologische Bundesanstalt, Wien.

Wagner, T., Fabel, D., Fiebig, M., Häuselmann, P., Sahy, D., Xu, S., Stüwe, K., 2010. Young uplift in the non-glaciated parts of the Eastern Alps. Earth and Planetary Science Letters, 295, 159–169. https://doi.org/10.1016/j.epsl.2010.03.034

Wagner, T., Fritz, H., Stüwe, K., Nestroy, O., Rodnight, H., Hellstrom, J., Benischke, R., 2011. Correlations of cave levels, stream terraces and planation surfaces along the river Mur-Timing of landscape evolution along the eastern margin of the Alps. Geomorphology, 134/1–2, 62–78.https://doi.org/10.1016/j.geomorph.2011.04.024

Weiss, E.H., 1977. Zur Hydrogeologie des Grundwasseraustrittes der Gurk unterhalb der Prekowa (Tiebelursprung). Carinthia II, 167/87, 95–104.

Whipple, K.X., Tucker, G.E., 1999. Dynamics of the stream-power river incision model: Implications for height limits of mountain ranges, landscape response timescales, and research needs. Journal of Geophysical Research: Earth Surface, 104/B8, 17,661–17,674. https://doi.org/10.1029/1999JB900120

Winkler-Hermaden, A., 1955. Ergebnisse und Probleme der Quartären Entwicklungsgeschichte am östlichen Alpensaum außerhalb der Vereisungsgebiete. Österreichische Akademie der Wissenschaften, Mathematisch-Naturwissenschaftliche Klasse, Denkschriften, 110, pp. 180.

Winkler-Hermaden, A., 1957. Geologisches Kräftespiel und Landformung. Springer, Wien, pp. 822.

Wobus, C., Whipple, K.X., Kirby, E., Snyder, N., Johnson, J., Spyropolou, K., Crosby, B., Sheehan, D., 2006. Tectonics from topography: Procedures, promise, and pitfalls. Geological Society of America, 398, 55–74. https://doi.org/10.1130/2006.2398(04)

Wölfler, A., Kurz, W., Fritz, H., Stüwe, K., 2011. Lateral extrusion in the Eastern Alps revisited: Refining the model by thermochronological, sedimentary, and seismic data. Tectonics, 30/4, 1–15. https://doi.org/10.1029/2010TC002782

Wölfler, A., Stüwe, K., Danisik, M., Evans, N.J., 2012. Low temperature thermochronology in the Eastern Alps: Implications for structural and topographic evolution. Tectonophysics, 541–543, 1–18. https://dx.doi.org/10.1016%2Fj.tecto.2012.03.016

Zeilinger, G., Kuhlemann, J., Reinecker, J., Kazmer, M., Frisch, W., 1999. Das Tamsweger Tertiär im Lungau (Österreich): Fazies und Deformation eines intramontanen Beckens. Neues Jahrbuch für Geologie und Paläontologie—Abhandlungen, 214/3, 537–569.

Received: 27 01 2019
Accepted: 21 07 2019

Thorsten BARTOSCH[1)*)] & Kurt STÜWE[1)]

[1)] Institute of Earth Sciences, University of Graz, Universitätsplatz 2, A-8010, Graz, Austria

[*)] Corresponding author: thorsten.bartosch@uni-graz.at